Table 1. Comparison of clinicopathological features of patients (n = 246) with HCC with and without K19 expression

Features	K19 >5% (n = 10)	K19 ≤5% (n = 236)	p value
Mean age ± SD, years	70 ± 8	68 ± 8	0.541
Sex, male/female	2/8	146/90	0.016
Clinical and laboratory data			
Mean AFP, ng/ml	489 [52.1]	12 [16.2]	0.062
Mean DCP, mAU/ml	42 [25]	321 [22]	0.773
Child-Pugh score A/B	8/2	200/36	0.655
Total bilirubin, mg/dl	0.9 ± 0.5	0.8 ± 0.4	0.480
Albumin, g/dl	3.4 ± 0.7	3.6 ± 0.5	0.137
PT, %	97 ± 12	92 ± 15	0.375
Pathology			
Tumor size, mm	24 ± 7	22 ± 8	0.392
Tumor number	1.3 ± 0.7	1.2 ± 0.6	0.891
Vascular invasion, yes/no	0/10	0/236	
Tumor differentiation well/moderate/poor	0/8/2	108/126/2	<0.0001
TNM stage I/II	8/2	183/53	0.855
Lymph node involvement yes/no	0/10	0/236	
Metastasis, yes/no	0/10	0/236	
Major associated liver diseases			
HBsAg+	1 (10)	24 (10.1)	0.895
HCV Ab+	9 (90)	189 (80.1)	
ALD	0	8 (3.4)	
NASH	0	2 (0.8)	
Unknown etiology	0	13 (5.6)	

Figures in parentheses are percentages; figures in brackets are medians. PT = Prothrombin time; HBsAg = hepatitis B surface antigen; HCV Ab = HCV antibody; ALD = alcoholic liver disease; NASH = non-alcoholic steatohepatitis.

Table 2. Comparison of the image findings of patients with HCC with and without K19 expression

	K19 positive >5% (n = 10)	K19 negative (n = 236)	p value
CECT arterial phase high density	10/10	200/235	0.187
CTHA high density	7/7	159/181	0.326
CTAP low density	7/7	179/181	0.779
SPIO-MRI T2*	10/10	175/184	0.473
EOB-MRI			
Hepatobiliary phase low intensity	–	46/47	–

proportional hazards model to assess their value as independent predictors.

All statistical analyses were performed using StatView (version 5.0) software (Abacus Concepts, Berkeley, Calif., USA).

Results

Proportion of HCCs Expressing K19

The biopsy number was 272, and the median length of our biopsy specimens was 8.2 ± 4.0 mm. In 117 cases, the specimens were <1 cm, and ≥1 cm in 155 cases. Pathological diagnosis and K19 staining were practicable in all specimens <1 cm. Expression of K19 in >5% of tumor cells was observed in HCCs from 10 of 246 patients (4.1%). Two of the 10 HCCs (20.0%) were poorly differentiated, and 8 (80.0%) were moderately differentiated. None of the well-differentiated HCCs showed K19 positivity. Among the 10 patients with K19-positive HCCs, 2 had a HCC nodule >3 cm and 8 had HCC nodules ≤3 cm in diameter. The 8 HCC nodules with K19 positivity ≤3 cm in diameter were moderately (n = 7) and poorly differentiated HCCs (n = 1).

Clinicopathological Characteristics of Patients with HCC in Relation to Expression of K19

The clinicopathological characteristics of the patients in relation to K19 expression in HCCs are shown in table 1. The proportion of well-differentiated HCCs was significantly lower among K19-positive HCC patients ($p < 0.0001$). K19 expression was more frequent among female than among male patients ($p = 0.016$). There were no significant differences in age, clinical laboratory data, tumor size, number of tumor nodules, tumor stage in TNM classification or etiology between K19-positive and -negative HCC patients. There was no significant difference in tumor location (near the major vessels, bile ducts and organs) between K19-positive and -negative patients. The number of RFA sessions did not differ significantly between K19-positive and -negative HCC patients. Serum AFP before initial RFA was not evaluated in 1 patient.

Imaging Characteristics of HCCs in Relation to Expression of K19

Comparison of the various imaging findings, according to vascular profiling, and in relation to K19 expres-

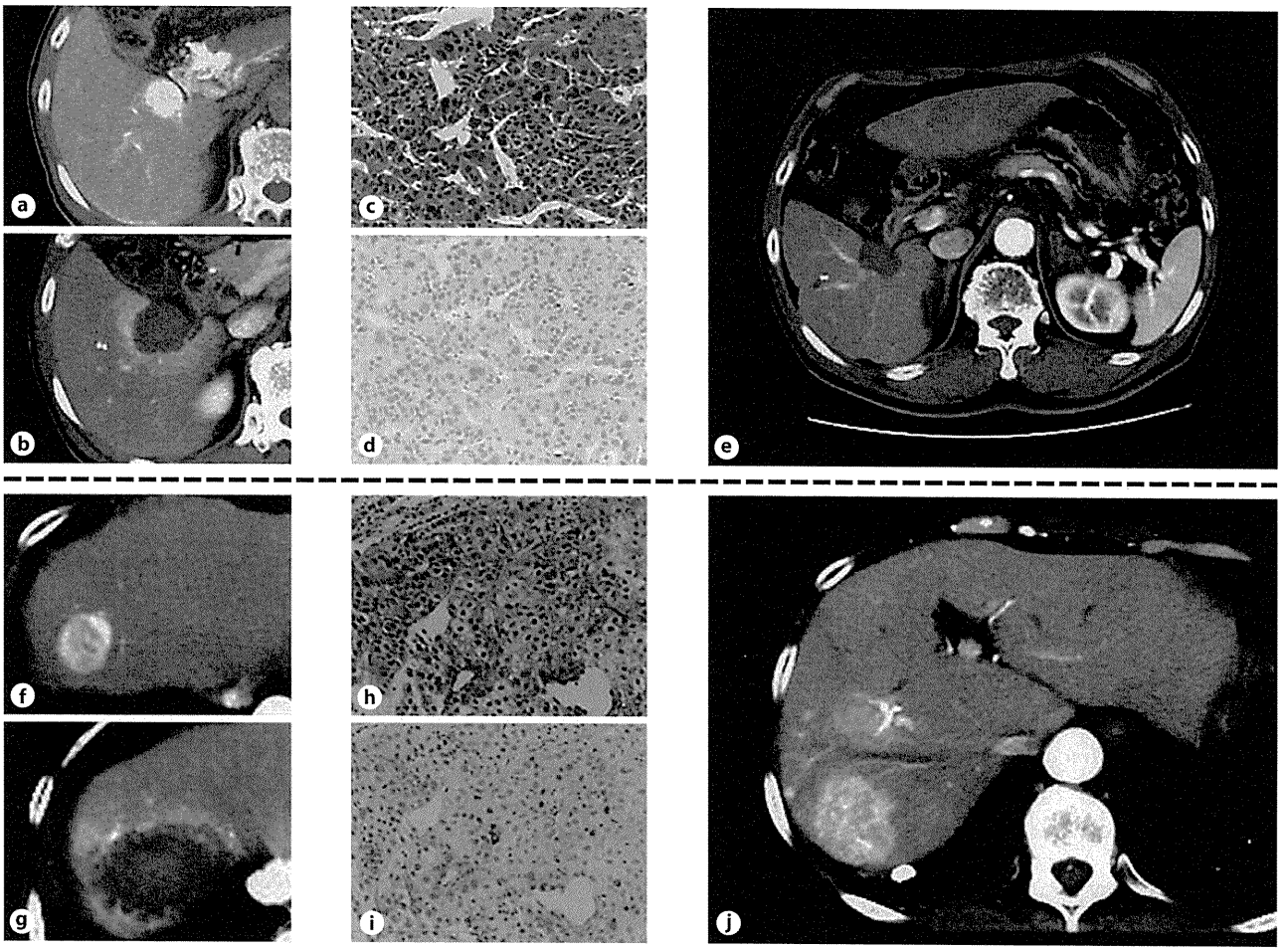

Fig. 2. a–e A patient with K19-negative HCC: a 70-year-old man with chronic hepatitis (anti-HCV positive). The HCC (25 mm in diameter, in segment 6) showed an early enhancement area by dynamic CT (**a**). Dynamic CT at 1 day after RFA (**b**). On histological investigation, the tumor showed moderately differentiated HCC on H&E staining (**c**), and K19 expression was negative in tumor cells (**d**). The HCC did not show early enhancement on dynamic CT 4 years and 10 months after curative RFA (**e**). **f–j** A patient with K19-positive HCC: a 72-year-old female with chronic hepatitis (anti-HCV positive). The HCC (25 mm in diameter, in segment 8) showed an early enhancement area by dynamic CT (**f**). CT 1 day after RFA (**g**). On histological investigation, the tumor showed moderately differentiated HCC on H&E staining (**h**), and K19-positive cells were seen in the tumor (**i**). Five months after RFA, the HCC showed intrahepatic recurrence beyond the Milan criteria (**j**).

sion, is shown in table 2. These imaging findings were consistent with the histological diagnosis, as determined by pretreatment needle biopsy.

All K19-positive HCCs showed typical HCC images, such as hypervascularity at the arterial phase, hypovascularity at the portal and equilibrium phases in dynamic CT, and hyperintensity at the T2* image in SPIO-MRI. There was no significant difference between K19-positive and -negative patients in terms of the imaging findings.

Recurrence of HCC after RFA

The median follow-up period was 34.0 months (range 65 days to 10.3 years). A recurrence of HCC was diagnosed at least once during the follow-up period in 156 patients (63.4%). The cumulative recurrence-free survival at 1, 3 and 5 years was 69.9, 26.6 and 12.2%, respectively. Among the 156 patients with recurrent HCC, 14 (8.9%) had local tumor progression and 142 (91.1%) had distant intrahepatic recurrences. Five of 14 patients (35%) who had local tumor progression had K19-positive HCC and

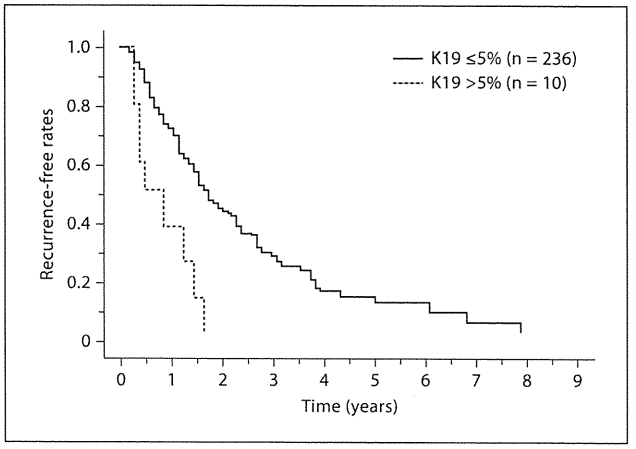

Fig. 3. The cumulative recurrence-free survival rate in patients with K19-positive (>5%) HCC was significantly lower than that in patients with K19-negative HCC (p = 0.0001).

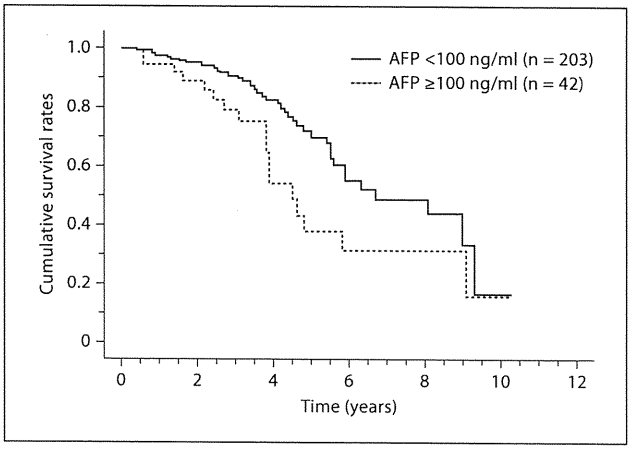

Fig. 4. The cumulative overall survival rate in patients with AFP ≥100 ng/ml was significantly lower than that in patients with AFP <100 ng/ml (p = 0.026).

3 of 5 patients with K19-positive HCC (60%) showed vascular invasion at the local tumor progression. Nine of 10 patients (90.0%) with K19-positive HCC had recurrences after initial treatment and 6 of 10 (60.0%) were detected within 1 year of initial curative RFA. On the other hand, 147 of 236 patients (62.2%) with K19-negative HCC had recurrences, and only 58 patients (24.5%) had recurrences within 1 year after RFA. There were no patients with K19-negative HCC who showed vascular invasion at the local tumor progression. Patients with K19-positive HCC were more likely to have an early recurrence of HCC (<1 year after RFA) than patients with K19-negative HCC (p = 0.012). The typical cases are shown in figure 2. The median recurrence-free survival in patients with K19-positive HCC was 194 days (range 93–635), while in patients with K19-negative HCC it was 446 days (range 65–2,978). Patients with K19-positive HCC had a significantly shorter recurrence-free survival than patients with K19-negative HCC (p = 0.0001) (fig. 3). The recurrence type, local tumor progression or distant intrahepatic recurrence differed between K19-positive and -negative patients. Local tumor progression was significantly higher in K19-positive patients than in K19-negative patients (p < 0.0001). Table 3 shows the results of univariate and multivariate analyses of prognostic factors for recurrence-free survival. In the multivariate analysis, K19 expression, the number of HCC nodules and total bilirubin ≥2 mg/dl were significant independent risk factors for HCC recurrence in all patients.

The percentage of distant metastasis and major portal invasion (VP3–4) was significantly higher in K19-positive than in K19-negative patients (p < 0.0001). Distal metastasis was detected in the lung (2 patients) and lymph node (1 patient), and major portal invasion was detected in 3 patients.

Risk Factors for Poor Prognosis

There was no patient who received liver transplantation in this study. Fifty-seven of 246 patients (23.1%) died during the follow-up period. The cause of death was progression of HCC in 37 patients, hepatic failure in 16 patients and causes unrelated to the liver in 4 patients. The overall survival rates for all patients were 97.2, 88.7 and 63.4% at 1, 3 and 5 years, respectively. A serum AFP level ≥100 ng/ml (p = 0.034), a total bilirubin level ≥2 mg/dl (p < 0.0001) and female sex (p = 0.018) were identified as risk factors for a poor prognosis in HCC in both univariate and multivariate analyses (table 4). Patients with high serum AFP levels (≥100 ng/ml) had significantly lower overall survival rates than patients with low serum AFP levels (p = 0.026) (fig. 4).

On the other hand, age (≥65 years), albumin concentration (≤3.5 g/dl), prothrombin time (≤70%), DCP (≥100 mAU/ml), tumor size, the number of HCC nodules and K19 expression were not significant risk factors for poor prognosis in the univariate analysis (table 4).

Table 3. Risk factors associated with recurrence-free survival in 246 patients with HCC after complete ablation by RFA

Risk factor	Univariate			Multivariate		
	RR	95% CI	p	RR	95% CI	p
Age <65 years	1.43	1.02–2.02	0.037	1.28	0.90–1.81	0.163
Sex, female	1.24	0.90–1.71	0.162			
Total bilirubin ≥2 mg/dl	2.50	1.02–6.25	0.034	2.70	1.08–6.66	0.032
Albumin ≤3.5 g/dl	1.12	0.81–1.56	0.492			
PT ≤70%	1.28	0.73–2.22	0.394			
AFP ≥100 ng/m	1.42	0.95–2.12	0.087			
DCP ≥100 mAU/ml	1.08	0.68–1.69	0.790			
Tumor size >3.0 cm	1.08	0.70–1.69	0.713			
2 or 3 tumor nodules	2.29	1.58–3.33	<0.0001	2.28	1.56–3.32	<0.0001
K19 positive (>5%)	3.57	1.75–7.14	0.0004	3.44	1.72–7.14	0.0005

RR = Risk ratio; CI = confidence interval; PT = prothrombin time.

Table 4. Risk factors associated with poor prognosis in 246 patients with HCC after complete ablation by RFA

Risk factor	Univariate			Multivariate		
	RR	95% CI	p	RR	95% CI	p
Age <65 years	1.19	0.68–2.09	0.527			
Sex, female	2.03	1.18–3.46	0.009	1.92	1.11–3.30	0.018
Total bilirubin ≥2 mg/dl	12.5	4.54–33.3	<0.0001	10.0	3.70–33.3	<0.0001
Albumin ≤3.5 g/dl	1.25	0.71–2.17	0.450			
PT ≤70%	1.49	0.59–3.84	0.674			
AFP ≥100 ng/ml	1.88	1.06–3.44	0.030	1.88	1.05–3.33	0.034
DCP ≥100 mAU/ml	1.06	0.53–2.12	0.880			
Tumor size >3.0 cm	1.12	0.44–1.78	0.730			
2 or 3 tumor nodules	1.23	0.67–2.26	0.492			
K19 positive (>5%)	1.29	0.46–3.57	0.632			

RR = Risk ratio; CI = confidence interval; PT = prothrombin time.

Risk Factors for Exceeding the Milan Criteria after RFA

Patients with K19-positive HCC exceeded the Milan criteria within 16.8 months. Multivariate analyses showed that K19 expression, high levels of DCP (≥100 mAU/ml), tumor number and total bilirubin ≥2 mg/dl were significant risk factors for tumor status exceeding the Milan criteria after curative RFA (table 5; fig. 5).

Complications

Most patients had mild pain or discomfort during RFA. Intraperitoneal hemorrhage and biloma were not seen in any patient. None of the patients developed dissemination of HCC, or skin or peritoneal metastases. There was no fatal complication.

Percentage of K19 Stain

We also analyzed another percentage of K19 stain (>1%). Thirteen of 246 patients had K19-positive (>1%) HCC and 12 of 13 patients with K19-positive (>1%) HCC had recurrences beyond the Milan criteria. Nine of 12 (75.0%) were detected with recurrence of HCC within 1 year of initial curative RFA. The final results were the same for K19 positivity (>5 and >1%, respectively). The

Table 5. Risk factors associated with exceeding the Milan criteria in 246 patients with HCC after complete ablation by RFA

Risk factor	Univariate			Multivariate		
	RR	95% CI	p	RR	95% CI	p
Age <65 years	1.63	1.08–2.45	0.018	1.17	0.75–1.83	0.463
Sex, female	1.16	0.78–1.72	0.457			
Total bilirubin ≥2 mg/dl	2.94	1.05–8.33	0.039	3.57	1.25–10.0	0.017
Albumin ≤3.5 g/dl	0.97	0.64–1.47	0.857			
PT ≤70%	0.89	0.41–1.96	0.763			
AFP ≥100 ng/ml	2.17	1.38–3.44	0.0008	1.56	0.96–2.50	0.077
DCP ≥100 mAU/ml	2.32	1.42–3.70	0.0007	2.08	1.26–3.44	0.004
Tumor size >3.0 cm	1.03	0.61–1.72	0.914			
2 or 3 tumor nodules	2.98	1.91–4.64	<0.0001	3.05	1.91–4.88	<0.0001
K19 positive (>5%)	3.70	1.81–7.69	0.0003	2.47	1.19–5.18	0.016

RR = Risk ratio; CI = confidence interval; PT = prothrombin time.

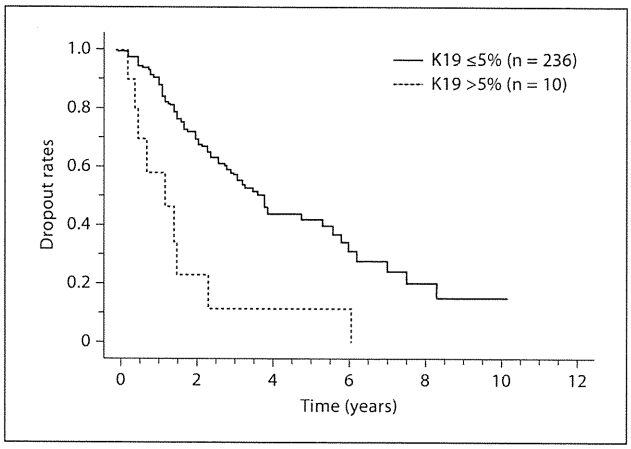

Fig. 5. The cumulative rate of exceeding the Milan criteria in patients with K19-positive HCC was significantly higher than that in patients with K19-negative HCC ($p < 0.0001$).

rate of recurrence and dropout from the Milan criteria were significantly higher in the patients with K19-positive (>1%) than in the patients with K19-negative HCC (data not shown).

Discussion

RFA therapy for HCC has been shown to achieve excellent results in appropriately selected patients [2–5]. However, recurrence of tumors is a serious impediment to improving the prognosis for patients treated with curative RFA. Therefore, several factors have been investigated as potential predictive markers for recurrence after curative RFA [7–9]. Recently, K19 was proposed as an independent prognostic factor for HCC [11–14]. However, these investigations were performed on surgically resected cases only and not on tumor biopsies. Although tumor biopsy is controversial because of potential complications such as tumor seeding [22], it would be beneficial to clinicians and patients to predict the individual tumor characteristics from a biopsy. Until now, the relationship between K19 expression and tumor recurrence after RFA treatment has not been assessed. Therefore, we have investigated the relationship between K19 expression in tumor biopsies and the clinicopathological findings in HCC. In this study, we investigated K19 expression in biopsy specimens taken just prior to the RFA session, and K19 expression (>5%) was demonstrated in 10 of 246 patients (4.1%). Because most of our patients were in early stage (within the Milan criteria) and 108 of 246 patients (43.9%) had well-differentiated HCC, the positive rate of K19 stain in our study was lower than that in surgical specimens.

We also analyzed another percentage of K19 stain (>1%) and the final results were the same for K19 positivity (>5 and >1%, respectively). K19 expression (>1%) was a statistically significant independent predictor for recurrence of HCC after RFA. Although the amount of tissue obtained by tumor biopsy is small compared to resected material, present data suggest that even biopsy can provide meaningful data on tumor recurrence irrespective of the percentage of K19 positivity (1 or 5%) (online sup-

plementary tables 1 and 2; for supplementary material see www.karger.com/doi/10.1159/000328448).

K19 positivity was not an independent predictor of the overall rate of survival, and serum AFP (≥100 ng/ml), total bilirubin (≥2 mg/dl) and female sex were significant independent predictors of survival. It is suggested that the level of total bilirubin affects the liver function of the patient, and liver function is one of the most important prognostic factors for survival of HCC patients.

The average age of our patients in this study was 68 ± 8 years, and no patients received liver transplantation in this study. However, liver transplantation is the most desirable treatment for HCC worldwide. Because of the prolonged waiting time for liver transplantation, RFA has been considered a safe and effective bridging therapy to liver transplantation. In addition, pretransplant RFA in patients with HCC has been considered for downstaging of HCC, thus improving the patient's survival [6, 7, 23]. In this study, K19 expression of HCC was a significant independent predictor for exceeding the Milan criteria ($p = 0.016$). In fact, 9 of 10 patients with K19-positive HCC exceeded the Milan criteria within 16.8 months. Therefore, if RFA is considered as a bridging therapy session prior to liver transplantation, it would be useful to obtain information on K19 expression in tumor tissue by performing a tumor biopsy before RFA. Therefore, careful observation for early detection of recurrence should be considered if K19-positive HCC patients are awaiting liver transplantation.

Compared to surgical specimens, biopsies taken prior to RFA may present some difficulties with regard to histological investigation. Needle biopsies of the nodules are less often indicated when typical vascular imaging of HCC is obtained, compared to hypovascular nodules. Needle tract seeding should also be considered. Needle biopsy has played an important role in making a diagnosis in the past. Recently, more reliance has been placed on the vascular imaging profile, because of its sensitivity and specificity without the risk of tumor dissemination. In addition, in comparison to recent advances in imaging, the information obtained from liver biopsy is lacking, as these only provide simple histological characterization, such as tumor differentiation [24]. Moreover, the positive predictive value of the vascular profile on dynamic imaging for diagnosis of HCC exceeds 95% [25]. Therefore, the current tendency is to consider needle biopsy as non-essential for diagnosis. However, in this study, K19-positive HCC showed exactly the same imaging findings as K19-negative HCC, suggesting that it is difficult to distinguish between these tumor types by imaging profile alone. In addition, K19-positive, moderately and/or poorly differentiated HCC showed similar cytological and structural abnormalities to K19-negative HCC, indicating that K19 positivity is unpredictable without staining. In figure 2, we present an impressive comparison of the features of K19-positive and -negative HCC, showing that, although the histology was similar, the prognosis for these patients was completely different. From these findings, it is clear that immunohistochemistry for K19 is the only way of demonstrating its positivity. Fortunately, staining for K19 on paraffin sections is common in diagnostic pathology, and it is not a problem to add this to routine hematoxylin and eosin (H&E) staining. Moreover, even for a general pathologist with no liver specialization, evaluating K19 expression should not be difficult, as long as care is taken not to count bile ducts, which may be associated with the remains of portal tracts. Taken together, these finding could indicate that it may be beneficial to check tumors for K19 positivity prior to RFA. Further research is warranted in larger groups to validate these findings and outweigh the potential additional clinical benefit compared to the potential risk of tract seeding during percutaneous biopsy.

Although biopsy has an important role in understanding the biological characteristics of HCC [26], tumor seeding by needle biopsy should be avoided. In practice, this is a major concern with needle biopsy of tumors. A review of tumor seeding following therapeutic procedures in HCC indicated that seeding occurred in 0–12.5% of cases (median 0.95%, mean 2.5%) [22]. As the time between biopsy and the treatment procedure was not specified, it is difficult to identify the factors that could have caused seeding. In the present study, tumor biopsies were performed just before RFA, using a needle-guiding technique, and tumor seeding was not observed. The same puncture line was used for both tumor biopsy and RFA, allowing complete ablation of the tumor using the tumor biopsy route. This may be one of the reasons it was possible in this study to biopsy the tumors without dissemination or bleeding. After treatment by RFA, the tumor cannot be investigated for histological features and K19 expression; therefore, we recommend taking a biopsy just before RFA for predicting tumor behavior using K19 expression. This would be valuable to both the clinician and the patient.

The mechanism of K19-positive HCC remains unclear. The facts that K19-positive cells are present in HCCs and that these positive cells form a spectrum suggest that K19-positive HCC may have originated from hepatic progenitor cells. These hepatic progenitor cells,

which are liver-specific adult stem cells, have potential stem cell features such as proliferation and differentiation. Once a tumor takes on these phenotypes, K19-positive HCC can still preserve these stem cell phenotypes. Therefore, this could be a possible reason why K19-positive HCC shows aggressive behavior in comparison with K19-negative HCC. In fact, previous publications and our study confirm these features [27].

In conclusion, we successfully evaluated the positivity of K19 in biopsy specimens. K19-positive HCCs showed significantly more frequent recurrence after curative RFA than K19-negative tumors and positive staining of K19 in the cytoplasm of HCC is closely associated with early intrahepatic recurrence (<1 year) and dropout from the Milan criteria. On imaging, K19-positive HCC showed only typical HCC findings and it was difficult to distinguish between K19-positive and -negative HCC. Taken together, these findings could indicate that >5% K19 positivity in tumor biopsy tissue is important for predicting tumor recurrence, which is not possible by imaging. Because of the high risk of tumor recurrence in K19-positive HCC, close observation for early detection of recurrence should be required.

Acknowledgments

We thank Hiroshi Suzuki, Satoshi Kusakari and Yuko Hashimoto for their excellent technical assistance, which was indispensable to this study.

This study was supported by grants from the Japanese Ministry of Welfare, Health, and Labor.

Disclosure Statement

The authors have nothing to disclose. They have no affiliation with the manufacturers of the drugs used in this study and have not received funding from the manufacturers to support this research.

References

1 Bruix J, Sherman M: Management of hepatocellular carcinoma. Hepatology 2005;42:1208–1236.

2 Tateishi R, Shiina S, Teratani T, Obi S, Sato S, Koike Y, Fujishima T, Yoshida H, Kawabe T, Omara M: Percutaneous radiofrequency ablation for hepatocellular carcinoma. An analysis of 1000 cases. Cancer 2005;103:1201–1209.

3 Shiina S, Teratani T, Obi S, Sato S, Tateishi R, Fujishima T, Ishikawa T, Koike Y, Yoshida H, Kawabe T, Omata M: A randomized controlled trial of radiofrequency ablation with ethanol injection for small hepatocellular carcinoma. Gastroenterology 2005;129:122–130.

4 Kudo M: Radiofrequency ablation for hepatocellular carcinoma: updated review in 2010. Oncology 2010;78:113–124.

5 Choi D, Lim HK, Rhim H, Kim YS, Lee WJ, Paik SW, Koh KC, Lee JH, Choi MS, Yoo BC: Percutaneous radiofrequency ablation for early-stage hepatocellular carcinoma as a first-line treatment: long-term results and prognostic factors in a large single-institution series. Eur Radiol 2007;17:684–692.

6 Lu DS, Yu NC, Raman SS, Lassman C, Tong MJ, Britten C, Durazo F, Saab S, Han S, Finn R, Hiatt JR, Busuttil RW: Percutaneous radiofrequency ablation of hepatocellular carcinoma as a bridge to liver transplantation. Hepatology 2005;41:1130–1137.

7 Mazzaferro V, Battiston C, Perrone S, Pulvirenti A, Regalia E, Romito R, Sarli D, Schavo M, Garbagnati F, Marchiano A, Spreafico C, Camerini T, Mariani L, Miceli R, Andreola S: Radiofrequency ablation of small hepatocellular carcinoma in cirrhotic patients awaiting liver transplantation: a prospective study. Ann Surg 2004;240:900–909.

8 Izumi N, Asahina Y, Noguchi O, Uchihara M, Kanazawa N, Itakura J, Himeno Y, Miyake S, Sakai T, Enomoto N: Risk factors for distant recurrence of hepatocellular carcinoma in the liver after complete coagulation by microwave or radiofrequency ablation. Cancer 2001;91:949–956.

9 Fernandes ML, Lin CC, Lin CJ, Chen WT, Lin SM: Risk of tumour progression in early-stage hepatocellular carcinoma after radiofrequency ablation. Br J Surg 2009;96:756–762.

10 Roskams T, De Vos R, Van Eyken P, Myazaki H, Van Damme B, Desmet V: Hepatic OV-6 expression in human liver disease and rat experiments: evidence for hepatic progenitor cells in man. J Hepatol 1998;29:455–463.

11 Yang XR, Xu Y, Shi GM, Fan J, Zhou J, Ji Y, Sun HC, Qiu SJ, Yu B, Gao Q, He YZ, Qin WZ, Chen RX, Yang GH, Wu B, Lu Q, Wu ZQ, Tang ZY: Cytokeratin 10 and cytokeratin 19: predictive markers for poor prognosis in hepatocellular carcinoma patients after curative resection. Clin Cancer Res 2008;14:3850–3859.

12 Zhuang PY, Zhang JB, Zhu XD, Zhang W, Wu WZ, Tan YS, Hou J, Tang ZY, Qin LX, Sun HC: Two pathologic types of hepatocellular carcinoma with lymph node metastasis with distinct prognosis on the basis of CK19 expression in tumor. Cancer 2008;112:2740–2748.

13 Uenishi T, Kubo S, Yamamoto T, Shuto T, Ogawa M, Tanaka H, Tanaka S, Kaneda K, Hirohashi K: Cytokeratin 19 expression in hepatocellular carcinoma predicts early postoperative recurrence. Cancer Sci 2003;94:851–857.

14 Durnez A, Verslype C, Nevens F, Fevery J, Aerts R, Pirenne J, Lesaffre E, Libbrecht L, Desmet V, Roskams T: The clinicopathological and prognostic relevance of cytokeratin 7 and 19 expression in hepatocellular carcinoma. A possible progenitor cell origin. Histopathology 2006;49:138–151.

15 Sobin LH, Fleming ID: TNM Classification of Malignant Tumors, fifth edition (1997). Union Internationale Contre le Cancer and the American Joint Committee on Cancer. Cancer 1997;80:1803–1804.

16 Kudo M, Okanoue T: Management of hepatocellular carcinoma in Japan: consensus-based clinical practice manual proposed by the Japan Society of Hepatology. Oncology 2007;72(suppl 1):2–15.

17 Hirohashi S, Ishak K, Kojiro M, Wanless I, Theise N, Tsukuma H: Tumours of the liver and intrahepatic bile ducts; in Hamilton SR, Aaltonen LA (eds): Pathology and Genetics of Tumours of the Digestive System. Lyon, IARC Press, 2000, pp 157–202.

18 De Baere T, Rehim MA, Teriitheau C, Deschamps F, Lapeyre M, Dromain C, Boige V, Dromain C, Boige V, Ducreux M, Elias D: Usefulness of guiding needles for radiofrequency ablative treatment of liver tumors. Cardiovasc Intervent Radiol 2006;29:650–654.
19 Lorentzen T: A cooled needle electrode for radiofrequency tissue ablation: thermodynamic aspects of improved performance compared with conventional needle design. Acad Radiol 1996;3:556–563.
20 Goldberg SN, Gazelle GS, Solbiati L, Rittman WJ, Mueller PR: Radiofrequency tissue ablation: increased lesion diameter with a perfusion electrode. Acad Radiol 1996;3:636–644.
21 Komorizono Y, Oketani M, Sako K, Yamasaki N, Shibatou T, Maeda M, Kohara K, Shigenobu S, Ishibashi K, Arima T: Risk factors for local recurrence of small hepatocellular carcinoma tumors after a single session, single application of percutaneous radiofrequency ablation. Cancer 2003;97:1253–1262.
22 Stigliano R, Marelli L, Yu D, Davies N, Patch D, Burroughs AK: Seeding following percutaneous diagnostic and therapeutic approaches for hepatocellular carcinoma. What is the risk and the outcome? Seeding risk for percutaneous approach of HCC. Cancer Treat Rev 2007;33:437–447.
23 Brillet PY, Paradis V, Brancatelli G, Rangheard AS, Consigny Y, Plessier A, Durand F, Belghiti J, Sommacale D, Vilgrain V: Percutaneous radiofrequency ablation for hepatocellular carcinoma before liver transplantation: a prospective study with histopathologic comparison. AJR Am J Roentgenol 2006;186:S296–S305.
24 Pawlik TM, Gleisner AL, Anders RA, Assumpcao L, Maley W, Choti MA: Preoperative assessment of hepatocellular carcinoma tumor grade using needle biopsy: implications for transplant eligibility. Ann Surg 2007;245:435–442.
25 Bruix J, Sherman M, Llovet JM, Beaugrand M, Lencioni R, Burroughs AK, Christensen E, Pagliaro L, Colombo M, Rodes J, EASL Panel of Experts on HCC: Clinical management of hepatocellular carcinoma. Conclusions of the Barcelona-2000 EASL conference. European Association for the Study of the Liver. J Hepatol 2001;35:421–430.
26 Rockey DC, Caldwell SH, Goodman ZD, Nelson RC, Smith AD: Liver biopsy. Hepatology 2009;49:1017–1044.
27 van Sprundel RG, van den Ingh TS, Spee B: Keratin 19 marks poor differentiation and a more aggressive behavior in canine and human hepatocellular tumours. Comp Hepatol 2010;9:4.

Clinical Study

Oncology

Oncology 2010;79:229–237
DOI: 10.1159/000322374

Received: July 28, 2010
Accepted after revision: September 17, 2010
Published online: March 3, 2011

Significance of DNA Polymerase Delta Catalytic Subunit p125 Induced by Mutant p53 in the Invasive Potential of Human Hepatocellular Carcinoma

Kensaku Sanefuji Akinobu Taketomi Tomohiro Iguchi Keishi Sugimachi Toru Ikegami Yo-ichi Yamashita Tomonobu Gion Yuji Soejima Ken Shirabe Yoshihiko Maehara

Department of Surgery and Science, Graduate School of Medical Sciences, Kyushu University, Fukuoka, Japan

Key Words
Hepatocellular carcinoma · p53 · Invasion · POLD1

Abstract
Objective: To clarify the role of DNA polymerase delta in tumor progression, we examined the expression of its main catalytic subunit p125 encoded by *POLD1* in hepatocellular carcinoma (HCC) and human HCC cell lines. ***Methods:*** We examined the expression of p53 and p125 in HCC by using immunohistochemistry and Western blotting. Characteristic changes observed in human HCC cell lines after transfection were examined. ***Results:*** Immunohistochemical examination revealed positive staining of p125 in HCC cell nuclei, but few positively stained cells were observed in noncancerous tissues ($p < 0.0001$). p125 expression in specimens significantly correlated with cellular differentiation ($p = 0.0048$) and the degree of vascular invasion ($p = 0.0401$). It also significantly correlated with abnormal p53 expression. In vivo studies showed that p125 was upregulated in mutant p53-transfected HepG2 cells, which had more invasive potential than did control cells. Furthermore, the expression and invasive potential were reduced by the silencer sequence for *POLD1*. ***Conclusions:*** These findings suggest that the DNA polymerase delta catalytic subunit p125 induced by mutant type p53 plays an important role in tumor invasion, which leads to a poorer prognosis in HCC.

Introduction

The alpha, delta, and epsilon types of mammalian DNA polymerase are essential for DNA replication [1]. DNA polymerase delta and epsilon regulate the synthesis of the leading and lagging strands, while DNA polymerase alpha is involved in primer synthesis [2] and processes of eukaryotic DNA repair [3, 4]. DNA polymerase delta and epsilon are distinguished from other mammalian DNA polymerases by their intrinsic 3′ to 5′ exonuclease activity which allows them to replicate DNA with high fidelity [5]. DNA polymerase delta replicates a large portion of the genome, synthesizing most of the lagging strand and perhaps contributing to leading-strand synthesis [6, 7].

KARGER

Fax +41 61 306 12 34
E-Mail karger@karger.ch
www.karger.com

0030–2414/10/0794–0229$26.00/0

Accessible online at:
www.karger.com/ocl

Akinobu Taketomi, MD, PhD
Department of Surgery and Science, Graduate School of Medicine, Kyushu University
3-1-1 Maidashi, Higashi-ku, Fukuoka 812-8582 (Japan)
Tel. +81 92 642 5466, Fax +81 92 642 5482
E-Mail taketomi@surg2.med.kyushu-u.ac.jp

The DNA polymerase delta complex consists of 4 subunits: p125, p68, p50, and p12 [8]. The polymerase and the 3′ to 5′ exonuclease active sites of polymerase delta reside in the p125 subunit, which is a 125-kDa protein encoded by *POLD1* in human cells [9]. The *POLD1* promoter is activated by the transcriptional factors Sp1 and Sp2 [9]. Its promoter is also suppressed by wild-type p53 which binds to p53 and recognizes a specific consensus DNA sequence [10]. Sp1 and p53 binding sites overlap each other, and *POLD1* promoter activity therefore appears to be regulated by competition between Sp1 and p53 binding to the site.

The p53 tumor suppressor gene is the most commonly altered protein discovered to date and its product functions as a checkpoint in maintaining genome stability [11]. Inactivation of the p53 gene is essentially due to small mutations that lead to the expression of a mutant protein. The p53 protein is induced and activated in response to various stimuli such as DNA damage or the expression of several oncogenes. p53 activation leads to 1 of 2 major cellular pathways, either apoptosis or cell cycle arrest, which prevents cells from progressing to the S phase until the damaged DNA is fully repaired. p53 recognizes a specific consensus DNA sequence, 5′-PuPuPuC(A/T)(T/A)GPyPyPy-3′, as a transcriptional factor [12].

Hepatocellular carcinoma (HCC) is the fifth most common cancer worldwide and the third most common cause of cancer mortality [13]. Despite recent progress in surgical techniques and postoperative management, the recurrence rates after the surgical resection of HCC remain high [14–17]. p53 overexpression was associated with the histological characteristics of HCC, such as poor cellular differentiation, tumor size, vascular invasion, and poor prognosis [18–21]. It is induced by mutations of the p53 gene, which induce conformational changes to stabilize the protein [22, 23]. These mutations were detected in 27% of HCCs and correlated with cellular differentiation and progression [24].

The following findings were recently reported: (1) defective proofreading of DNA polymerase delta induced a high incidence of epithelial cancers in mice [25]; (2) a *POLD1* variant was associated with an approximately 2-fold increase in the relative risk of breast cancer [26]; (3) the hot spots for the loss of a heterozygosity or allelic imbalance of *BRCA1/2*-related breast cancers harbor *POLD1* [27], and (4) intentional mutation at the polymerase active site of DNA polymerase delta increases genomic instability and accelerates tumorigenesis [28]. DNA polymerase delta is therefore thought to play a crucial role in tumor progression. To clarify the role of DNA polymerase delta in liver cancer, we examined p125 expression in HCC and human HCC cell lines and assessed the characteristic changes in human HCC cell lines observed after transfection and the RNA interference-mediated silencing of p125.

Materials and Methods

Cell Cultures

Three established human lines of HCC and HeLa cells (Riken Cell Bank, Tsukuba, Japan) differing in p53 status were used in this study. Huh7 cells have p53 mutations at codon 220 [29], p53 is deleted in Hep3B cells [30], and HepG2 cells contain wild-type p53 [30]. HeLa cells contain human papilloma virus and wild-type p53. In HeLa cells, any p53 that is synthesized is rapidly degraded by E6 protein, which reduces the level of that protein to 0 [31]. All cells were cultured in DMEM (Life Technologies, Inc.) supplemented with 10% fetal bovine serum, 500 U/ml penicillin, and 500g μg/ml streptomycin (Life Technologies, Inc.), and maintained at 37°C in 5% CO_2.

Patients and Specimens

Tissue samples were obtained from 82 Japanese patients who underwent curative hepatectomy for primary HCC without preoperative treatment at Kyushu University Hospital between 1995 and 2001 and provided preoperative written informed consent. This study conformed to the ethical guidelines of the 1975 Declaration of Helsinki as reflected in a priori approval by the appropriate institutional review committee. All tumors were defined as HCC, and pathological features of the tumors were determined histologically according to the General Rules for the Clinical and Pathological Study of Primary Liver Cancer of the Liver Cancer Study Group of Japan [32].

Quantitative Real-Time Polymerase Chain Reaction

To analyze the mRNA expression, quantitative real-time polymerase chain reactions (qRT-PCR) were performed with a LightCycler® 2.0 system using a Universal Probe Library approach with LightCycler TaqMan Master (Roche, Tokyo, Japan) and appropriate Universal Probes [UPL Probe No. 67 for *POLD1* and No. 60 for glyceraldehyde 3-phosphate dehydrogenase *(GAPDH)*; Roche], according to the manufacturer's instructions. *GAPDH* was used as the internal control. Specific amplification of the target sequence was obtained using primers designed by Probe Finder software (Roche) to amplify *POLD1* (NM_002691.1) or *GAPDH* (NM_002046.3). To verify that the correct targets were amplified, PCR products were run on an agarose gel and visualized with ethidium bromide staining on an ultraviolet transilluminator. The primer sequences for *POLD1* and *GAPDH* were 5′-CCCTACGTGATCATCAGTGC-3′ (forward primer for *POLD1*), 5′-AGGTAGTACTGCGTGTCAATGG-3′ (reverse primer for *POLD1*), 5′-AGCCACATCGCTCAGACA-3′ (forward primer for *GAPDH*), and 5′-GCCCAATACGACCAAATCC-3′ (reverse primer for *GAPDH*).

Western Blot

To analyze protein expression, SDS-PAGE and Western blot were performed using an Invitrogen™ NuPAGE® Novex® Bis-Tris MiniGel system (Invitrogen, Tokyo, Japan) according to the manufacturer's instructions. Normalized protein lysates were boiled in electrophoresis SDS sample buffer, run on a 10% SDS-PAGE gel, and transferred onto a polyvinylidine difluoride membrane (Invitrogen). The primary antibodies used in this study were against p125 (1:200 dilution, mouse monoclonal antibody, clone A-9; Santa Cruz Biotechnology, Inc., Santa Cruz, Calif., USA), p53 (1:1,000 dilution, mouse monoclonal antibody, clone DO-7; Dako, Tokyo, Japan), and β-actin (1:1,000 dilution, mouse monoclonal antibody, clone AC-15; Sigma Aldrich, Tokyo, Japan). Cases in which the relative p125 expression level in the tumor lesion was more than 0.5 [the upper 95% confidence interval (CI) limit of the relative p125 expression level in noncancerous tissues] were considered high-expression cases and the others were considered low-expression cases.

Immunohistochemical Staining

Immunohistochemical observations were performed on adjacent deparaffinized sections using the EnVision™+ System-horseradish peroxidase method (Dako). The primary antibodies used in this study were against p125 (1:300 dilution, rabbit polyclonal antibody, clone H-300; Santa Cruz Biotechnology) and p53 (1:100 dilution, mouse monoclonal antibody, clone DO-7; Dako). Immunohistochemical staining was examined under a light microscope by 2 pathologists. Sections with nuclear staining for p53 in >10% cells were considered positive [20]. Cases in which nuclear staining for p125 was greater in the tumor lesion than in noncancerous tissues were considered high-expression cases and the others were considered low-expression cases.

Invasion Assay

The invasive potential was determined in a Matrigel invasion assay using polycarbonate membranes (pore size 8.0 μm) in the upper chamber of 24-well Transwell culture chambers coated with Matrigel (Becton Dickinson Co., Tokyo, Japan) according to the manufacturer's instructions and as previously described [33]. Cell lines (2.0×10^4 cells/well) suspended in 500 μl DMEM without fetal bovine serum were placed in the upper chamber, and the lower chamber was filled with 750 μl DMEM along with 20% fetal bovine serum as a chemoattractant. Inserts without Matrigel were used as the control. The cells were allowed to migrate through Matrigel for 36 or 72 h. The membranes were stained using a Diff-Quik staining kit (Siemens Healthcare Diagnostics, Inc., Deerfield, Ill., USA). The number of invading cells was expressed as an invasion percentage, i.e. the mean number of cells invading through the Matrigel insert membrane divided by the mean number of cells migrating under the control insert membrane. Each experiment was performed in triplicate.

Plasmid Construction

A p53 Dominant-Negative Vector Set and a pIRES2-AcGFP1 Vector were purchased from Clontech Laboratories, Inc. (Takara Bio). The coding sequence for p53mt135 was ligated into the *Sac*I and *Eco*RI sites of the pIRES2-AcGFP1 vector to generate pIRES2-AcGFP1-p53mt135. The plasmid constructs was confirmed by direct sequence analysis. The pIRES2-AcGFP1-null vector was used as the control. When p53mt135 and p53 are co-expressed, they form a mixed tetramer that is unable to interact with p53-binding sites, thereby blocking the downstream effects of p53 [34, 35].

Stable Transfection

One microgram of plasmid construct was transfected into HepG2 cells using FuGENE® 6 Transfection Reagent (Roche) according to the manufacturer's instructions and as previously described [36]. The transfected cells were selected for resistance to 1,000 μg/ml of G418 (Roche) for 6 weeks. Stably transfected pIRES2-AcGFP1-p53mt135 was confirmed to strongly express p53 by Western blot and by the detection of green fluorescent cells.

RNA Interference

For silencing experiments, cells were transfected with small interfering RNA (siRNA) duplexes using an X-tremeGENE siRNA transfection reagent (Roche), according to the manufacturer's instructions, and harvested 72 h after transfection to obtain the protein. Two siRNAs were purchased from Ambion, Inc. (Applied Biosystems, Tokyo, Japan). Silencer® Negative Control #1 siRNA was used as the negative control. The silencer sequence for *POLD1* was 5′-CCUUCAUCCGUAUCAUGGAtt-3′ (Silencer Select pre-designed siRNA, siRNA ID s614).

Statistical Analysis

Univariate survival analysis was performed using the Kaplan-Meier method and results were compared by univariate logrank and Wilcoxon tests. Metric variables were compared with independent samples by a nonparametric Wilcoxon test. Nominal variables were compared using Fisher and χ^2 tests, and they were compared with multivariate data using multivariate logistic regression analysis. $p < 0.05$ was considered statistically significant. All statistical analyses were performed using JMP 6.0 software for Macintosh (SAS Institute, Inc., Cary, N.C., USA).

Results

p125 Expression in Human HCC

Since p125 expression in clinical samples has not been analyzed before, preliminary analyses of p125 expression levels in human HCC were conducted. Sixty-seven clinical samples (28 noncancerous and 39 cancerous) were examined by Western blot (fig. 1a). p125 expression was significantly higher in human HCC than in noncancerous tissues (fig. 1b; $p < 0.0001$). Immunohistochemistry was performed to identify the cellular localization of p125 in hepatocytes and to determine its expression levels (fig. 1c). There was immunochemical p125 staining in cancer cell nuclei. Few positively stained cells (<1%) were observed in noncancerous tissues. These results show that p125 expression was higher in cancerous tissues than in noncancerous tissues.

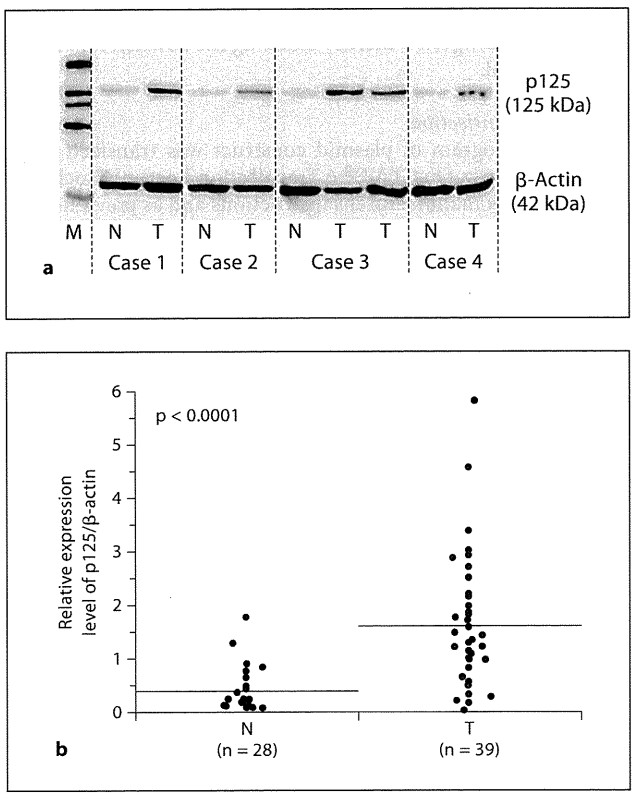

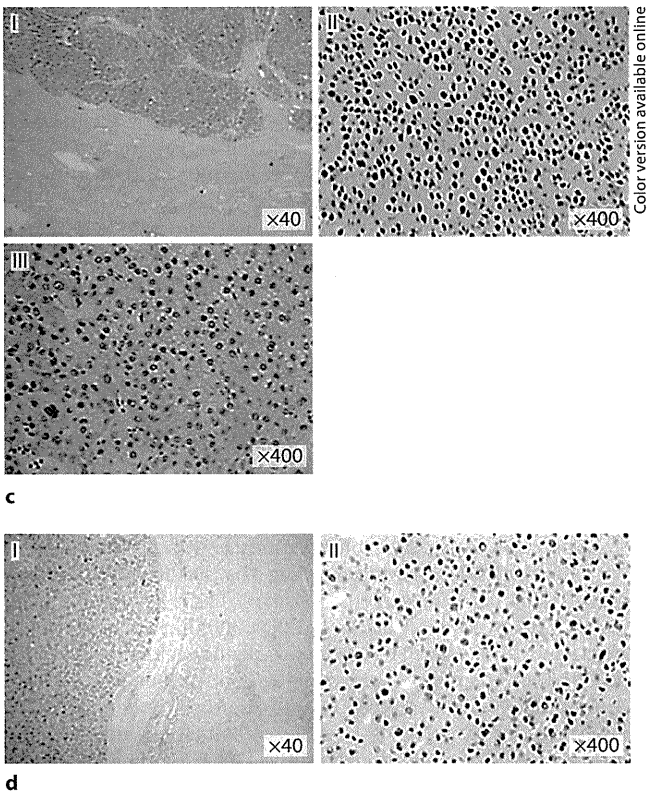

Fig. 1. Immunological expression of p125 and p53 in human HCC. **a** Western blot analysis of p125 in human HCC. Each lane was loaded with 20 μg total protein. **b** Scatter diagram showing the p125 distribution determined by quantitative Western blot in paired normal and tumor liver tissue samples. The relative mean expression level of p125 was 0.38 (95% CI 0.22–0.54) in noncancerous tissues and 1.59 (95% CI 1.19–1.99) in cancerous tissues. **c** Immunohistochemistry for p125. Cases with high p125 expression are shown in I. A cancerous lesion of a case with high p125 expression is shown in II. A cancerous lesion of a case with low p125 expression is shown in III. **d** Immunohistochemistry for p53. A cancerous lesion of a case with p53-positive staining is shown. β-Actin was used as the internal control. M = Marker; N = surrounding normal tissue; T = tumor tissue.

Relationship between the Expression of p125 and POLD1 mRNA

To examine the correlation between the expression of p125 and *POLD1* mRNA, 64 cases were divided into high-expression (n = 46) and low-expression (n = 18) groups based on immunohistochemical findings. mRNA expression was significantly higher in the high-expression group than in the low-expression group (p = 0.0126; fig. 2a). Forty-three cases were divided into 25 high-expression and 18 low-expression cases by Western blot. mRNA expression was significantly higher in high-expression cases than in low-expression cases (p = 0.0164; fig. 2b). These results indicate that p125 expression correlated with *POLD1* mRNA expression.

Relationship between the Expression of p125 and p53

To examine the correlation between the expression of p125 and p53, a total of 82 cases were divided into high-expression (n = 59) and low-expression (n = 23) groups based on immunohistochemical findings for p125. p53 was also stained immunochemically in nuclei (fig. 1d). p53 expression significantly correlated with p125 expression (p = 0.02; fig. 2c). We also examined the p53 mutation of exons 5–8 in 79 cases by direct sequence analysis, excluding 3 cases in which DNA was not available. Immunohistochemical staining of p53-positive cases (47 cases) showed a significantly high p53 mutation rate (28%) compared with p53-negative cases (32 cases, 0%; data not shown). These findings indicate that high p125 expression was associated with abnormal p53 expression.

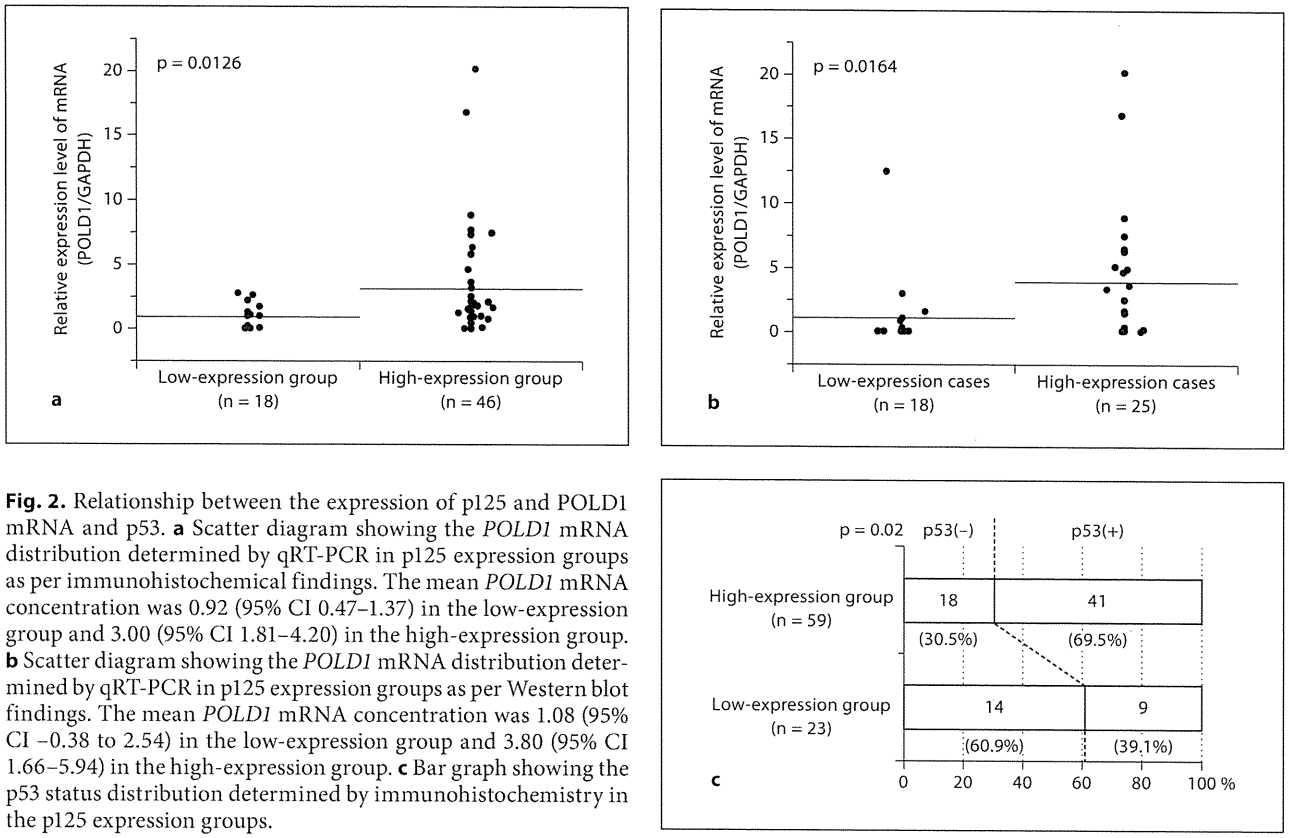

Fig. 2. Relationship between the expression of p125 and POLD1 mRNA and p53. **a** Scatter diagram showing the *POLD1* mRNA distribution determined by qRT-PCR in p125 expression groups as per immunohistochemical findings. The mean *POLD1* mRNA concentration was 0.92 (95% CI 0.47–1.37) in the low-expression group and 3.00 (95% CI 1.81–4.20) in the high-expression group. **b** Scatter diagram showing the *POLD1* mRNA distribution determined by qRT-PCR in p125 expression groups as per Western blot findings. The mean *POLD1* mRNA concentration was 1.08 (95% CI –0.38 to 2.54) in the low-expression group and 3.80 (95% CI 1.66–5.94) in the high-expression group. **c** Bar graph showing the p53 status distribution determined by immunohistochemistry in the p125 expression groups.

Relationship between Immunohistochemical Results, Clinicopathological Features, and Survival

Table 1 shows a comparison of clinicopathological features between patients with tumors expressing high (high-expression group, n = 59) and low (low-expression group, n = 23) p125 levels. p125 expression significantly correlated with gender, the indocyanine green 15-min retention rate, operation time, resection volume, anatomic resection, serum alpha-fetoprotein levels, serum des-gamma-carboxyl prothrombin levels, pathological differentiation, grade, vascular invasion, and intrahepatic metastasis. To examine the association between p125 expression and pathological features, logistic regression for qualitative variables was performed with adjustment for tumor size, tumor number, vascular invasion, intrahepatic metastasis, pathological differentiation, and grade. Backward stepwise multivariate logistic regression analysis revealed that the high p125 expression correlated with poor histological differentiation (p = 0.0048) and positive vascular invasion (p = 0.0401). Survival and disease-free survival were compared between the high- and low-expression groups. The disease-free survival curves of the high- and low-expression groups showed significant separation (p = 0.0496 by Wilcoxon's test; fig. 3).

Relationship between p125 Expression, p53 Expression, and the Invasive Potential of HCC Cell Lines

p125 expression was detected in all HCC cell lines and HeLa cells using Western blot (fig. 4a). Huh7 cells expressed lower p125 levels and higher p53 levels compared with HeLa, HepG2, and Hep3B cells. In p53-deleted Hep3B and rapidly degraded HeLa cells, higher p125 levels were observed. p125 expression and p53 expression were inversely correlated. The invasive potential of those cells was examined using a Matrigel invasion assay (fig. 4b). Huh7 cells exhibited significantly less invasive potential than did the other cell lines ($p < 0.05$). These findings indicate that the invasive potential of HCC cell lines correlated with p125 expression.

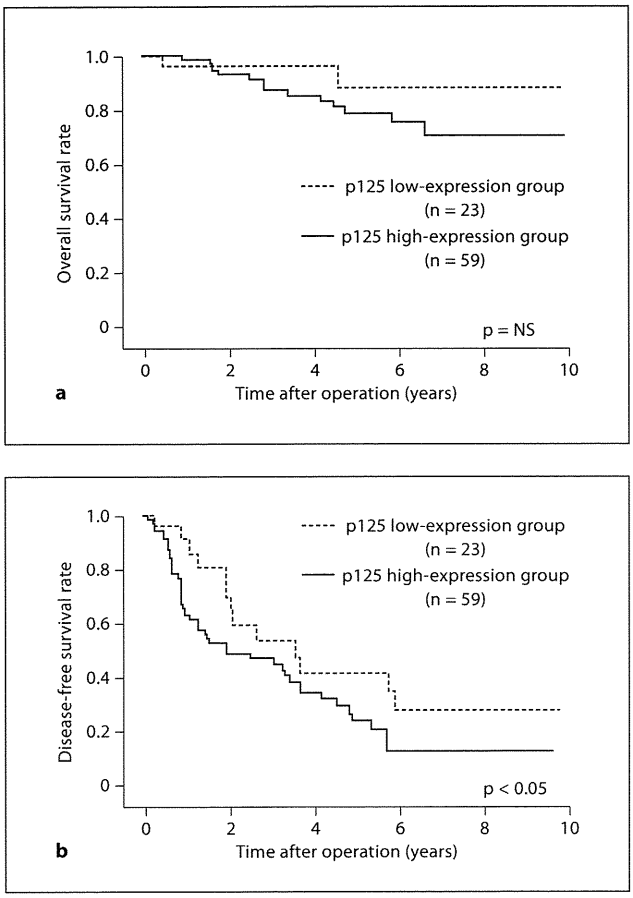

Fig. 3. Survival curves according to p125 expression level. **a** Overall survival curves for HCC patients having tumors with high (solid line) and low expressions (dotted line) of p125 (p = NS). **b** Disease-free survival curves for the high- (solid line) and low-expression (dotted line) groups ($p < 0.05$, Wilcoxon's test).

Table 1. Comparison of clinicopathological features between HCC patients with tumors showing high and low p125 expressions

Variables	p125 expression level		
	low-expression group (n = 23)	high-expression group (n = 59)	p value
Clinical factors			
Age[1], years	65.4 ± 8.5	63.5 ± 9.8	NS
Male/female ratio	22/1	43/16	<0.05
Positive HBs-Ag, %	8.7	20.3	NS
Positive HCV-Ab, %	60.9	66.1	NS
Total protein[1], g/dl	7.2 ± 0.7	7.2 ± 0.7	NS
Albumin[1], g/dl	3.82 ± 0.32	3.85 ± 0.42	NS
AST[1], U/l	52.6 ± 31.2	57.4 ± 25.3	NS
ALT[1], U/l	60.2 ± 41.3	65.8 ± 49.4	NS
Total bilirubin[1], mg/dl	0.81 ± 0.25	0.86 ± 0.33	NS
Platelets[1], $\times 10^4/\mu l$	14.0 ± 4.84	14.2 ± 7.9	NS
PT[1], %	84.8 ± 17.6	82.5 ± 12.2	NS
ICG-R15[1], %	19.5 ± 8.5	15.3 ± 9.0	<0.05
Child's classification (B and C), %	17.4	11.9	NS
Surgical factors			
Operation time[1], min	281 ± 56	330 ± 97	<0.05
Resection volume[1], g	152 ± 153	295 ± 335	<0.05
Anatomical resection, %	26.1	55.9	<0.05
Estimated blood loss[1], g	813 ± 639	1,015 ± 904	NS
Transfusion (+), %	13.0	11.9	NS
Tumor factors			
log[AFP (ng/ml)][1]	1.26 ± 0.88	1.76 ± 1.17	<0.05
log[DCP (mAU/ml)][1]	1.88 ± 0.73	2.39 ± 1.04	<0.05
Tumor size[1], cm	3.04 ± 1.84	4.31 ± 3.12	NS
Tumor number (multiple), %	34.8	44.1	NS
Stage 3 and 4, %	47.8	50.9	NS
Grade 3, %	4.4	28.8	<0.05
Poor histology, %	4.4	30.5	<0.05
Vascular invasion (+), %	0	22.0	<0.05
i.m. (+), %	8.7	32.2	<0.05

[1]Mean ± standard deviation.

HBs-Ag = Hepatitis B virus antigen; HCV-Ab = hepatitis C virus antibody; AST = aspartate aminotransferase; ALT = alanine aminotransferase; PT = prothrombin time; ICG-R15 = indocyanine green 15-min retention test; AFP = alpha-fetoprotein; DCP = des-gamma-carboxyl prothrombin; i.m. = intrahepatic metastasis.

Alteration of the Invasive Potential of HepG2 and p125 Expression

To investigate whether cellular invasiveness was regulated by p125 expression, stable transfection experiments using the induced exogenous dominant negative mutant p53mt135 were performed in HepG2 cells containing wild-type p53. The dominant negative mutant p53mt135 increased p125 expression (fig. 5a). Transfection of the control vector did not affect p125 expression or the invasive potential of HepG2 cells. The latter significantly increased with p125 expression (p = 0.0003; fig. 5b). RNA interference experiments were performed in stably transfected pIRES2-AcGFP1-p53mt135 HepG2 cells using the silencer sequence for *POLD1*. p125 expression was decreased by silencing for *POLD1* transfection (fig. 5c). Negative control siRNA transfection had no effect on p125 expression or its invasive potential. The invasive potential of HepG2 cells was significantly decreased with p125 expression (p = 0.0003; fig. 5d). These findings indicate that the invasive potential directly correlated with p125 expression.

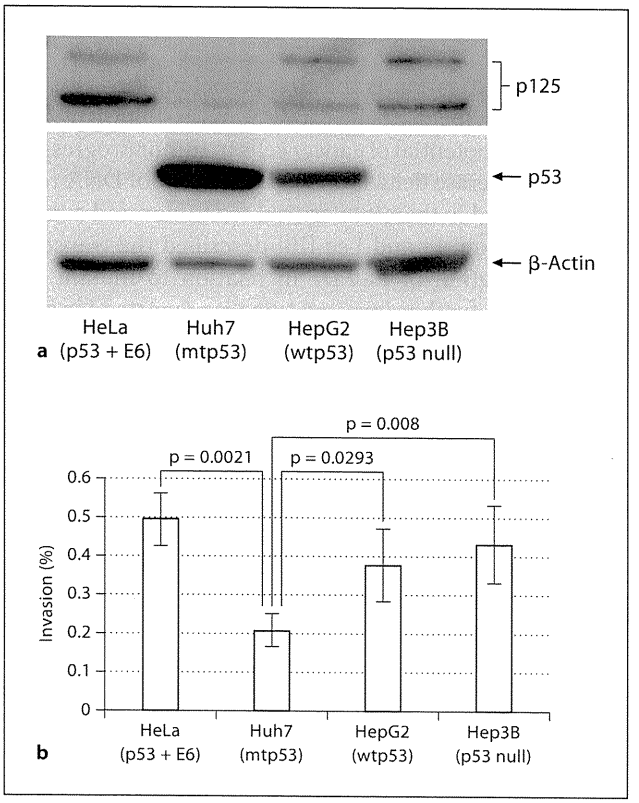

Fig. 4. Relationship between p125 expression, p53 expression, and the invasive potential of HCC cell lines. **a** Western blot of p125 and p53. Each lane was loaded with 20 μg total protein. **b** Invasive potentials were determined by the Matrigel invasion assay. Each experiment was performed in triplicate.

Fig. 5. Alteration of the invasive potential of HepG2 and p125 expression. **a**, **c** Western blot of p125 and p53. Each lane was loaded with 20 μg total protein. **b**, **d** The invasive potential was determined in the Matrigel invasion assay. **b** The mean invasion percentage of nontreated HepG2 cells was set to 1.00 and the invasive potential of stably transfected HepG2 cells is represented as a fraction. **d** The invasion percentage of nontreated stably transfected HepG2 pIRES2-AcGFP1-null cells was calculated as 1.00 and the invasive potential is represented as a fraction. Each experiment shown in **b** and **d** was performed in triplicate.

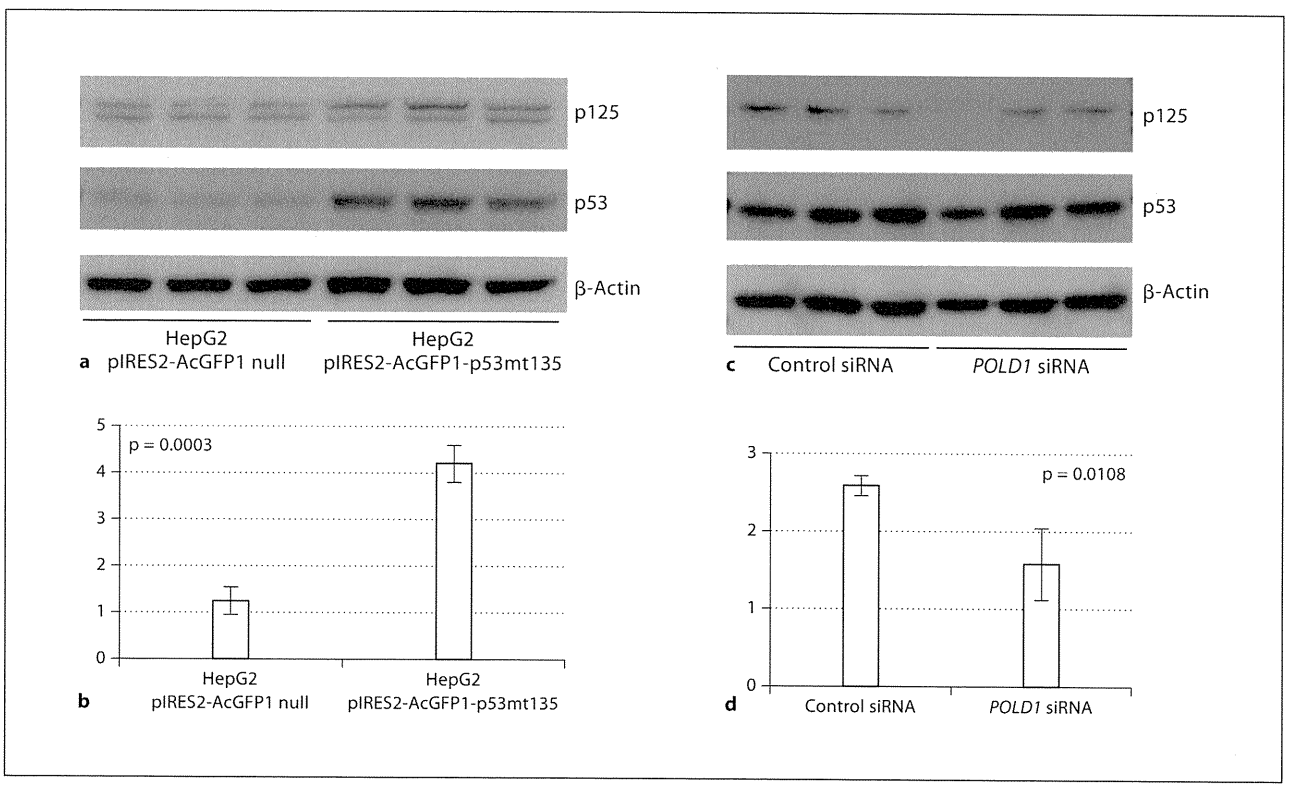

Discussion

This investigation is the first report on the impact of the DNA polymerase delta catalytic main subunit p125 on the invasive potential of cancer cells in tumor progression. DNA polymerase delta is an essential agent of DNA replication [1] and is therefore crucial for tumor and somatic cell replication. Li and Lee [10] described the transcriptional regulation of *POLD1* in relation to mutant p53. However, no further investigation was reported for some time. In this study, we found that the p125 induced by mutant p53 plays an important role in tumor invasion and contributes to the cellular differentiation of human HCC. Those findings were limited to the early stage of HCC and not necessarily to more advanced stages where those findings may differ, so further investigation was needed.

Wild-type p53 is generally not detected by immunohistochemical staining because of its short half-life. Mutations of the p53 gene may induce conformational changes that stabilize the protein, resulting in the accumulation of nuclear p53 that is detectable by immunohistochemical staining [22, 23]. p53 mutation analysis revealed that immunohistochemical staining of p53-positive cases had a significantly high p53 mutation rate compared with p53-negative cases. Immunohistochemical staining of p53 was therefore thought to be an abnormal protein that is induced by p53 mutation. In our study, immunohistochemical staining revealed a relationship between p125 and p53 expression; especially in heterozygously stained multiple nodular-type HCC, the staining pattern of p53 was the same as that of p125. This is consistent with some previous findings in which a promoter assay of *POLD1* showed that it was suppressed by wild-type p53 or activated by a mutant type of p53 that blocks the binding of wild-type p53 to a specific sequence [10]. These results suggest that p125 expression in HCC is regulated by transcription induced by abnormal p53. A correlation between the expression profile of p53 and the degree of differentiation has been reported [20, 37]. These reports support our finding that p125 might contribute to tumor cell dedifferentiation. The amount of p125 correlated with mRNA levels, suggesting that p125 overexpression in HCC is regulated by transcription.

We performed further investigations using HCC cell lines to investigate whether cellular invasiveness is regulated by p125 expression. There was an inverse correlation between p125 and p53 expression in Huh7, HepG2, and Hep3B cells. We tried to reveal the alteration of the invasive potential of Huh-7 by wild-type p53 stable transfection. Despite repeated transfection experiments, however, we could not establish a sufficient number of wild-type p53 stably transfected Huh-7. Both wild- and mutant-type p53 were detected by mouse monoclonal antibody DO-7 in cell lysates [38]. Huh7 cells have a p53 mutation at codon 220 that induces abnormal p53 [29]. However, not all genes suppressed by wild-type p53 were upregulated in Huh7 cells [39]. Different p53 mutations could have different capacities to suppress target genes. p125 expression might not be affected by p53 mutations in Huh7 cells; hence, p125 may be normally suppressed by p53 in Huh7 cells. The invasive potential of HCC cell lines correlated with p125 expression. Furthermore, the exogenous mutant of p53 induced p125 and increased the invasive potential of HepG2 cells. Inversely, p125 expression and cellular invasive potential were reduced in the RNA interference assay. These findings were supported by immunohistochemical results showing that HCC with high p125 levels had a high rate of venous invasion and p53 overexpression.

The *POLD1* promoter has consensus sequences at the AP-1 and E2F binding sites. E2F is thought to be important for the promoter activity of *POLD1* [9]. Transcriptional activation by E2F is directly inhibited by the tumor suppressor gene pRB resulting from E2F-RB complex formation [40]. Therefore, p125 also might play an important role in tumor progression related to pRB-dependent carcinogenesis.

In conclusion, we demonstrated that p125 expression is upregulated in HCC characterized by venous invasion, poor cellular differentiation, and a poor prognosis. We also showed that the invasive potential of HCC cell lines increased with p125 expression induced by abnormal p53. Our results suggest that p125 induced by p53 mutation plays an important role in tumor invasion and contributes to the cellular differentiation of human HCC. The p125 subunit of the DNA polymerase catalytic domain is therefore a potential therapeutic target for human HCC.

Acknowledgments

We appreciate the advice and expertise of T. Maeda, T. Yoshizumi, N. Harada, D. Kitagawa, S. Itho, and H. Kayashima. We are also grateful to Y. Kubota for providing the paraffin sections and to T. Shishino and K. Yamashita for their laboratory assistance.

Disclosure Statement

This study was supported in part by a Grant-in-Aid for Scientific Research from the Japan Society for the Promotion of Science, Tokyo, Japan.

References

1 Hubscher U, Maga G, Spadari S: Eukaryotic DNA polymerases. Annu Rev Biochem 2002; 71:133–163.
2 Johnson A, O'Donnell M: Cellular DNA replicases: components and dynamics at the replication fork. Annu Rev Biochem 2005;74: 283–315.
3 Lydeard JR, Jain S, Yamaguchi M, Haber JE: Break-induced replication and telomerase-independent telomere maintenance require pol32. Nature 2007;448:820–823.
4 Maloisel L, Fabre F, Gangloff S: DNA polymerase delta is preferentially recruited during homologous recombination to promote heteroduplex DNA extension. Mol Cell Biol 2008;28:1373–1382.
5 Kunkel TA, Bebenek K: DNA replication fidelity. Annu Rev Biochem 2000;69:497–529.
6 Pavlov YI, Shcherbakova PV, Rogozin IB: Roles of DNA polymerases in replication, repair, and recombination in eukaryotes. Int Rev Cytol 2006;255:41–132.
7 Garg P, Burgers PM: DNA polymerases that propagate the eukaryotic DNA replication fork. Crit Rev Biochem Mol Biol 2005;40: 115–128.
8 Liu L, Mo J, Rodriguez-Belmonte EM, Lee MY: Identification of a fourth subunit of mammalian DNA polymerase delta. J Biol Chem 2000;275:18739–18744.
9 Zhao L, Chang LS: The human POLD1 gene: identification of an upstream activator sequence, activation by sp1 and sp3, and cell cycle regulation. J Biol Chem 1997;272: 4869–4882.
10 Li B, Lee MY: Transcriptional regulation of the human DNA polymerase delta catalytic subunit gene POLD1 by p53 tumor suppressor and sp1. J Biol Chem 2001;276:29729–29739.
11 Harris CC: P53 tumor suppressor gene: from the basic research laboratory to the clinic – an abridged historical perspective. Carcinogenesis 1996;17:1187–1198.
12 el-Deiry WS, Kern SE, Pietenpol JA, Kinzler KW, Vogelstein B: Definition of a consensus binding site for p53. Nat Genet 1992;1:45–49.
13 El-Serag HB, Rudolph KL: Hepatocellular carcinoma: epidemiology and molecular carcinogenesis. Gastroenterology 2007;132: 2557–2576.
14 Kubo S, Tanaka H, Takemura S, Yamamoto S, Hai S, Ichikawa T, Kodai S, Shinkawa H, Shuto T, Hirohashi K: Surgical treatment for hepatocellular carcinoma detected after successful interferon therapy. Surg Today 2007; 37:285–290.
15 Shirabe K, Takenaka K, Taketomi A, Kawahara N, Yamamoto K, Shimada M, Sugimachi K: Postoperative hepatitis status as a significant risk factor for recurrence in cirrhotic patients with small hepatocellular carcinoma. Cancer 1996;77:1050–1055.
16 Sanefuji K, Kayashima H, Iguchi T, Sugimachi K, Yamashita Y, Yoshizumi T, Soejima Y, Nishizaki T, Taketomi A, Maehara Y: Characterization of hepatocellular carcinoma developed after achieving sustained virological response to interferon therapy for hepatitis C. J Surg Oncol 2009;99:32–37.
17 Ueno M, Uchiyama K, Ozawa S, Nakase T, Togo N, Hayami S, Yamaue H: Prognostic impact of treatment modalities on patients with single nodular recurrence of hepatocellular carcinoma. Surg Today 2009;39:675–681.
18 Qin LX, Tang ZY, Ma ZC, Wu ZQ, Zhou XD, Ye QH, Ji Y, Huang LW, Jia HL, Sun HC, Wang L: P53 immunohistochemical scoring: an independent prognostic marker for patients after hepatocellular carcinoma resection. World J Gastroenterol 2002;8:459–463.
19 Caruso ML, Valentini AM: Overexpression of p53 in a large series of patients with hepatocellular carcinoma: a clinicopathological correlation. Anticancer Res 1999;19:3853–3856.
20 Hsu HC, Tseng HJ, Lai PL, Lee PH, Peng SY: Expression of p53 gene in 184 unifocal hepatocellular carcinomas: association with tumor growth and invasiveness. Cancer Res 1993;53:4691–4694.
21 Ng IO, Lai EC, Chan AS, So MK: Overexpression of p53 in hepatocellular carcinomas: a clinicopathological and prognostic correlation. J Gastroenterol Hepatol 1995;10: 250–255.
22 Iggo R, Gatter K, Bartek J, Lane D, Harris AL: Increased expression of mutant forms of p53 oncogene in primary lung cancer. Lancet 1990;335:675–679.
23 Baas IO, Mulder JW, Offerhaus GJ, Vogelstein B, Hamilton SR: An evaluation of six antibodies for immunohistochemistry of mutant p53 gene product in archival colorectal neoplasms. J Pathol 1994;172:5–12.
24 Tanaka S, Toh Y, Adachi E, Matsumata T, Mori R, Sugimachi K: Tumor progression in hepatocellular carcinoma may be mediated by p53 mutation. Cancer Res 1993;53:2884–2887.
25 Goldsby RE, Hays LE, Chen X, Olmsted EA, Slayton WB, Spangrude GJ, Preston BD: High incidence of epithelial cancers in mice deficient for DNA polymerase delta proofreading. Proc Natl Acad Sci USA 2002;99: 15560–15565.
26 Sigurdson AJ, Hauptmann M, Chatterjee N, Alexander BH, Doody MM, Rutter JL, Struewing JP: Kin-cohort estimates for familial breast cancer risk in relation to variants in DNA base excision repair, BRCA1 interacting and growth factor genes. BMC Cancer 2004;4:9.
27 Weber F, Shen L, Fukino K, Patocs A, Mutter GL, Caldes T, Eng C: Total-genome analysis of BRCA1/2-related invasive carcinomas of the breast identifies tumor stroma as potential landscaper for neoplastic initiation. Am J Hum Genet 2006;78:961–972.
28 Venkatesan RN, Treuting PM, Fuller ED, Goldsby RE, Norwood TH, Gooley TA, Ladiges WC, Preston BD, Loeb LA: Mutation at the polymerase active site of mouse DNA polymerase delta increases genomic instability and accelerates tumorigenesis. Mol Cell Biol 2007;27:7669–7682.
29 Hsu IC, Tokiwa T, Bennett W, Metcalf RA, Welsh JA, Sun T, Harris CC: P53 gene mutation and integrated hepatitis B viral DNA sequences in human liver cancer cell lines. Carcinogenesis 1993;14:987–992.
30 Bressac B, Galvin KM, Liang TJ, Isselbacher KJ, Wands JR, Ozturk M: Abnormal structure and expression of p53 gene in human hepatocellular carcinoma. Proc Natl Acad Sci USA 1990;87:1973–1977.
31 May E, Jenkins JR, May P: Endogenous HeLa p53 proteins are easily detected in HeLa cells transfected with mouse deletion mutant p53 gene. Oncogene 1991;6:1363–1365.
32 Liver Cancer Study Group of Japan: General Rules for the Clinical and Pathological Study of Primary Liver Cancer, ed 2. Tokyo, Kanehara, 2003.
33 Itoh S, Maeda T, Shimada M, Aishima S, Shirabe K, Tanaka S, Maehara Y: Role of expression of focal adhesion kinase in progression of hepatocellular carcinoma. Clin Cancer Res 2004;10:2812–2817.
34 Scheffner M, Takahashi T, Huibregtse JM, Minna JD, Howley PM: Interaction of the human papillomavirus type 16 E6 oncoprotein with wild-type and mutant human p53 proteins. J Virol 1992;66:5100–5105.
35 Vogelstein B, Kinzler KW: p53 function and dysfunction. Cell 1992;70:523–526.
36 Varnavski AN, Young PR, Khromykh AA: Stable high-level expression of heterologous genes in vitro and in vivo by noncytopathic DNA-based kunjin virus replicon vectors. J Virol 2000;74:4394–4403.
37 Donato MF, Arosio E, Del Ninno E, Ronchi G, Lampertico P, Morabito A, Balestrieri MR, Colombo M: High rates of hepatocellular carcinoma in cirrhotic patients with high liver cell proliferative activity. Hepatology 2001;34:523–528.
38 Vojtesek B, Bartek J, Midgley CA, Lane DP: An immunochemical analysis of the human nuclear phosphoprotein p53: new monoclonal antibodies and epitope mapping using recombinant p53. J Immunol Methods 1992; 151:237–244.
39 Vikhanskaya F, Lee MK, Mazzoletti M, Broggini M, Sabapathy K: Cancer-derived p53 mutants suppress p53-target gene expression – potential mechanism for gain of function of mutant p53. Nucleic Acids Res 2007;35:2093–2104.
40 Harbour JW, Dean DC: Rb function in cell-cycle regulation and apoptosis. Nat Cell Biol 2000;2:E65–E67.

Human Molecular Genetics, 2011, Vol. 20, No. 19 **3884–3892**
doi:10.1093/hmg/ddr301
Advance Access published on July 12, 2011

A genome-wide association study of chronic hepatitis B identified novel risk locus in a Japanese population

Hamdi Mbarek[1], Hidenori Ochi[2,3], Yuji Urabe[1], Vinod Kumar[1], Michiaki Kubo[2], Naoya Hosono[2], Atsushi Takahashi[2], Yoichiro Kamatani[1], Daiki Miki[2,3], Hiromi Abe[3], Tatsuhiko Tsunoda[2], Naoyuki Kamatani[2], Kazuaki Chayama[2,3], Yusuke Nakamura[1,2] and Koichi Matsuda[1,*]

[1]Laboratory of Molecular Medicine, Human Genome Center, Institute of Medical Science, The University of Tokyo, Tokyo, Japan, [2]Center for Genomic Medicine, RIKEN, Kanagawa, Japan and [3]Division of Frontier Medical Science, Department of Medicine and Molecular Science, Programs for Biomedical Research, Graduate School of Biomedical Sciences, Hiroshima University, Hiroshima, Japan

Received February 23, 2011; Revised June 23, 2011; Accepted July 7, 2011

Hepatitis B virus (HBV) infection is a major health issue worldwide which may lead to hepatic dysfunction, liver cirrhosis and hepatocellular carcinoma. To identify host genetic factors that are associated with chronic hepatitis B (CHB) susceptibility, we previously conducted a two-stage genome-wide association study (GWAS) and identified the association of *HLA-DP* variants with CHB in Asians; however, only 179 cases and 934 controls were genotyped using genome-wide single nucleotide polymorphism (SNP) arrays. Here, we performed a second GWAS of 519 747 SNPs in 458 Japanese CHB cases and 2056 controls. After adjustment with the previously identified variants in the *HLA-DP* locus (rs9277535), we detected strong associations at 16 loci with *P*-value of $<5 \times 10^{-5}$. We analyzed these loci in three independent Japanese cohorts (2209 CHB cases and 4440 controls) and found significant association of two SNPs (rs2856718 and rs7453920) within the *HLA-DQ* locus (overall *P*-value of 5.98×10^{-28} and 3.99×10^{-37}). Association of CHB with SNPs rs2856718 and rs7453920 remains significant even after stratification with rs3077 and rs9277535, indicating independent effect of *HLA-DQ* variants on CHB susceptibility (*P*-value of 1.52×10^{-21} – 2.38×10^{-30}). Subsequent analyses revealed *DQA1*0102-DQB1*0604* and *DQA1*0101-DQB1*0501* [odds ratios (OR) =0.16, and 0.39, respectively] as protective haplotypes and *DQA1*0102-DQB1*0303* and *DQA1*0301-DQB1*0601* (OR = 19.03 and 5.02, respectively) as risk haplotypes. These findings indicated that variants in antigen-binding regions of *HLA-DP* and *HLA-DQ* contribute to the risk of persistent HBV infection.

INTRODUCTION

Hepatitis B virus (HBV) is the most common cause of infectious liver diseases, and about 400 million people are suffering from chronic viral infection worldwide. Routes of infection include vertical transmission during neonatal period and horizontal transmission in childhood (bites, lesions and sanitary habits) or adulthood (sexual contact, drug use and medical exposure). In Japan, most of the chronic hepatitis B (CHB) patients were infected through vertical transmission and become HBV carrier (1). Nearly 90% of the HBV carrier will clear HBV (negative for HBsAg and positive for HBc ab) during adolescence, and only 10% of the HBV carrier indicate persistent liver dysfunction and develop chronic hepatitis (2). CHB dramatically increases the risk to progress to liver cirrhosis and hepatocellular carcinoma over a period of several decades (3,4). Currently, CHB is a serious public health problem worldwide, however pathogenesis of HBV-related diseases still remains elusive.

*To whom correspondence should be addressed at: Laboratory of Molecular Medicine, Institute of Medical Science, The University of Tokyo, 4-6-1, Shirokanedai, Minato, Tokyo 108-8639, Japan. Tel: +81 354495376; Fax: +81 354495123; Email: koichima@ims.u-tokyo.ac.jp

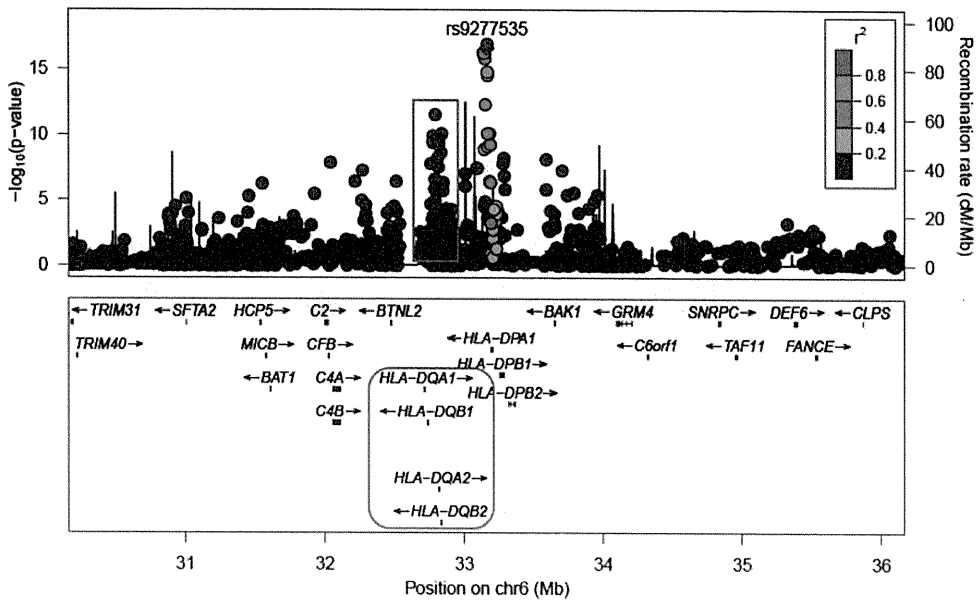

Figure 1. Signal of association with CHB in the *HLA* region of the GWAS stage. This figure shows the regional plots of the negative decadic logarithm trend *P*-values in a ~ 3000 kb window centered on the association peak, located at rs9277535 in *HLA-DPB1*. The top panel shows all SNPs in this region plotted according to the significance of their association with CHB and color coded according to their LD (r^2) with the most significant SNP, rs9277535 (see right corner of the plot). Vertical blue lines indicate local recombination rate. The bottom panel shows the genes in the region. The strongest signal on 6p21.32 localizes to *HLA-DP* genes and the second strongest signal localizes to *HLA-DQ* genes.

In addition to the viral and environmental factors, host genetic factors are considered to govern the pathology of disease development, progression or regression. Genetic epidemiological studies provide robust evidence that genetic variations contribute to progression from acute to chronic hepatitis (5). In 2009, our group conducted a genome-wide association study (GWAS) in the Asian population and identified a strong association of CHB with variants in the *HLA-DP* genes (6). In addition to our report, several association studies have suggested that genetic factors such as *HLA* (7–9), cytokines (10–12) and immune response-related genes (13–15) could influence the outcomes of HBV infection. However, these susceptibility loci were not identified in our previous study probably due to smaller sample size or smaller phenotypic effects of these loci. Here we conducted a second GWAS in the Japanese population to identify new susceptibility loci for CHB by increasing the number of samples in the screening stage from 179 cases and 934 controls to 458 case and 2056 controls.

RESULTS

We performed a two-stage GWAS followed by two independent replications as described in the Supplementary Material, Figure S1. In the GWAS stage, we genotyped 458 Japanese patients with CHB and 2056 control individuals using Illumina gene chip and obtained the genotyping results of 423 627 single nucleotide polymorphisms (SNPs) after quality control (QC). Examination of the quantile–quantile plots of the GWAS stage indicated no evidence for inflation of the test statistics, which could occur in the presence of population substructure ($\lambda = 1.028$) and also revealed an enrichment of significant *P*-values, suggesting the possible existence of candidates (Supplementary Material, Fig. S2A). The results of genome-wide association analysis are represented in Supplementary Material, Table S2, where a total of 34 SNPs in the major histocompatibility complex (MHC) region satisfied the genome-wide significance level ($P < 5.0 \times 10^{-8}$). We also found 54 SNPs (40 in the MHC region and 14 in the non-MHC region) with suggestive associations ($P < 5.0 \times 10^{-5}$) (Supplementary Material, Fig. S2B and Tables S2 and S3). We confirmed the most significant association at the *HLA-DP* locus as described in our previous report (rs9277535 and rs3077, $P = 3.72 \times 10^{-17}$ and 1.28×10^{-16}, respectively) (6) and found another significant peak around the *HLA-DQ* locus which is located ~300 kb telomeric to the *HLA-DP* locus (Fig. 1). To identify SNPs that are associated with CHB independently from *HLA-DP* SNPs, we conducted the association analysis after adjustment for a top SNP in the *HLA-DP* locus (rs9277535) using a logistic regression model (Fig. 2). As a result, five SNPs in the MHC region indicated suggestive associations ($P < 5.0 \times 10^{-5}$) even after stratification with rs9277535. Finally, 5 SNPs in the MHC region and 11 SNPs in the non-MHC region were selected for further analysis (Supplementary Material, Table S4).

Subsequently, we analyzed these 16 SNPs in the first replication set consisting of 606 cases and 2022 controls and found 2 SNPs within the MHC region [rs2856718, $P = 1.6 \times 10^{-5}$, odds ratios (OR) =1.33; rs7453920, $P = 5.72 \times 10^{-4}$, OR = 1.43] to be significantly associated with CHB after stratification for rs9277535 ($P_{corrected} < 3.0 \times 10^{-3}$, Supplementary Material, Table S5). The SNP rs2856718 is located in the intergenic region between *HLA-DQA2* and *HLA-DQB1*, while rs7453920 is located in intron 1 of *HLA-DQB2*

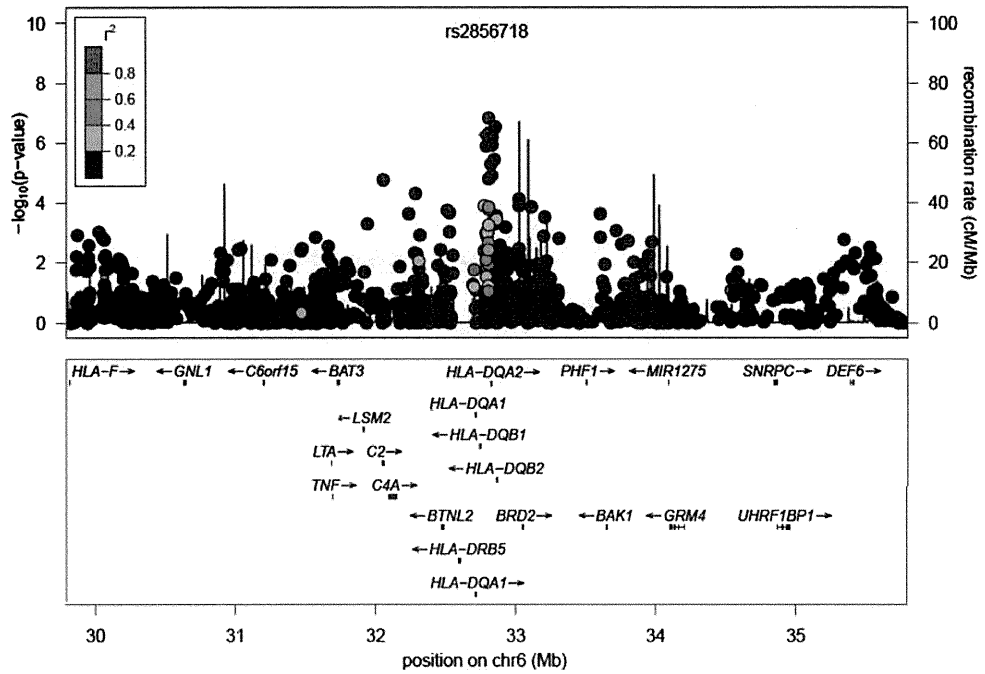

Figure 2. Regional association plot of the 6p21.32 locus after adjustment for the top SNP (rs9277535) in the *HLA-DP* locus in the GWAS stage. This figure shows the evidence of independent association with CHB based on logistic regression analysis. Only one strong peak remained after adjustment for rs9277535. This peak, represented by three top SNPs: rs3892710, rs7453920 and rs2856718, is located in the *HLA-DQ* locus (6p21.32).

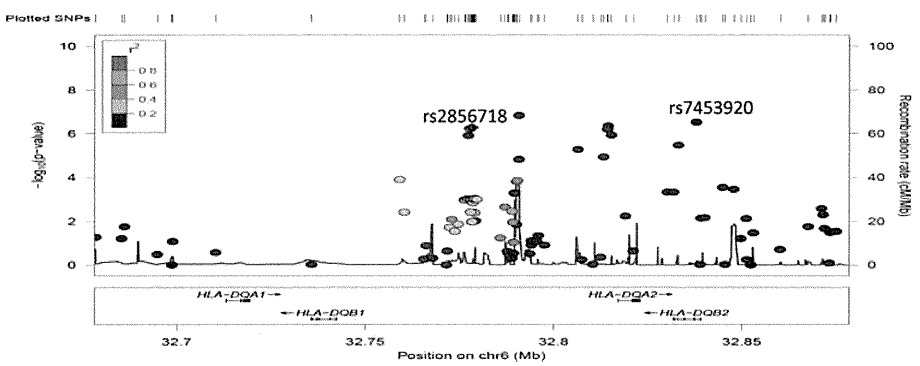

Figure 3. Regional association plot of the *HLA-DQ* locus. This figure indicates a ~200 kb region centered on the association peak, located between rs2856718 and rs7453920. The middle panel shows the genes in this region including the *HLA-DQ* locus.

(Fig. 3). To further validate these results, we analyzed these SNPs in two additional Japanese cohorts consisting of 381 cases and 1539 controls from Biobank Japan as well as 1222 cases and 879 controls from Hiroshima University. Association for these SNPs loci was confirmed in both replication sets (P-value $= 3.14 \times 10^{-5}$–3.59×10^{-12}; Table 1). To combine these studies, we conducted a meta-analysis with a fixed-effects model using the Mantel–Haenszel method. As shown in Table 1 and Supplementary Material, Figure S3, the OR were quite similar among the four studies and no heterogeneity was observed. Mantel–Haenszel P-values for independence were 3.99×10^{-37} for rs2856718 [OR = 1.77, 95% confidence interval (CI) = 1.65–1.91], and 5.98×10^{-28} for rs7453920 (OR = 1.81, 95% CI = 1.62–2.01). Two previously reported SNPs on the *HLA-DP* locus (rs9277535 on *HLA-DPB1* and rs3077 on *HLA-DPA1*) were also associated with CHB ($P_{\text{meta-analysis}} = 2.55 \times 10^{-54}$ and 1.57×10^{-61}) (Table 1).

To test whether the strong association observed in these regions is due to the effect of one of them, we performed logistic regression analysis based on the effect of each top SNP in both *HLA-DP* and *HLA-DQ* loci. Notably, rs2856718 and rs7453920 did show strong association with CHB after adjusting for the effect of rs3077 ($P = 8.12 \times 10^{-27}$ and $P = 1.52 \times 10^{-21}$, respectively) and rs9277535 ($P = 2.38 \times 10^{-30}$ and $P = 2.21 \times 10^{-22}$, respectively), indicating variants at the *HLA-DQ* locus are associated with CHB independent of the effect of *HLA-DP* polymorphisms (Table 2).